REPRINTED FROM:

Experimental Heat Transfer, Fluid Mechanics and Thermodynamics 1993

Volume 1

Proceedings of the Third World Conference on
Experimental Heat Transfer, Fluid Mechanics and Thermodynamics
Honolulu, Hawaii, USA, 31 October-5 November, 1993

Experimental Heat Transfer, Fluid Mechanics and Thermodynamics 1993
M.D. Kelleher et al. (Editors)

THE CHANGING ROLES OF EXPERIMENTAL AND COMPUTATIONAL FLUID MECHANICS

A.J. Strazisar

NASA Lewis Research Center, Cleveland, OH 44135 U.S.A.

1993
ELSEVIER
AMSTERDAM • LONDON • NEW YORK • TOKYO

Experimental Heat Transfer, Fluid Mechanics and Thermodynamics 1993
M.D. Kelleher et al. (Editors)

THE CHANGING ROLES OF EXPERIMENTAL AND COMPUTATIONAL FLUID MECHANICS

A.J. Strazisar

NASA Lewis Research Center, Cleveland, OH 44135 U.S.A.

ABSTRACT

When computational fluid mechanics was in its infancy, experiments and theoretical analysis were often the primary approaches used to study flow physics. Numerical simulations were performed after an experiment was complete, and the measured, theoretical, and numerical results were compared to assess the accuracy of the numerical results. As numerical simulation techniques have matured, computational, analytic, and experimental efforts have become equal partners in fluid mechanics research. Today numerical simulations are being used to guide the design of experimental hardware, to determine those areas of the flow field in which to concentrate the measurement effort, and to complement measurements in studying flow physics. The changing roles of experimental, analytical, and computational research will be traced by reviewing several investigations in which these approaches were used in varying degrees. A case will be made for maintaining a high degree of interaction between these approaches throughout the course of an investigation. The development of prototype computing systems designed to enhance the integration of numerical simulations and flow physics experiments will also be described.

INTRODUCTION

The importance of using experimental measurements, mathematical analysis, and numerical methods to investigate fluid mechanics problems has long been recognized. Most of us are introduced to this concept during our formal education. Graduate programs of study in fluid and thermal sciences include strong emphasis on pure and applied mathematics and, in more recent times, on numerical methods as well. Graduate students who perform an experiment for their dissertation research are often encouraged by their professors to either perform some analysis of the problem on their own or to compare their measured results with theoretical, analytic, or computational results generated by other researchers. Conversely, students who pursue an analytic approach to a problem are often encouraged to compare their results to experimental measurements in order to assess the accuracy of their results.

In our professional careers we tend to specialize in one approach or the other. This is in large part necessitated by the complexity of our experimental, theoretical, and numerical methods - it is a rare individual who is expert in all three. The field of fluid and thermal sciences has therefore been divided by natural forces into two "camps", experimental and theoretical/analytic/computational. In addition, the very organization of our research laboratories, in which there are quite often separate "test" and "numerical analysis" groups, continues to foster this situation. Because of these facts, the integration of experimental and computational approaches in a particular investigation is not something which naturally "happens" - it must be proactively sought by one camp or the other.

In the past, experimental and analytic approaches to problems were often done separately. The interaction between the two approaches consisted of comparing results when both efforts were complete, and learning from the results. This "open loop" way of doing business has changed markedly over the past forty years. I believe that this change has been driven by the significant advances which have occurred in both analysis and measurement capability. During this time, instrumentation has progressed from pitot probes and thermocouples to high-response instruments (such as hot-wires and semiconductor pressure transducers) and to non-intrusive optical techniques (such as laser anemometry and laser-based spectroscopy). Analysis approaches have moved from the realm of approximation methods to the realm of computational fluid mechanics, which in itself has moved from the solution of inviscid equations to the solution of the full three- dimensional Navier-Stokes equations. These advances now necessitate a new way of doing business, in which computations and experiments are conducted concurrently during an investigation. For example, the experimentalist needs to know "Where should I concentrate my measurements? Is there likely to be separated flow in the corner of the model?" The analyst can answer "Yes, I predict separation will occur, but I don't trust my transition model. Can you tell me where the flow separates? My predicted separation point varies as I change the parameters in my transition model and I'd like to know which settings yield the best agreement with your measurements".

The roles of analysis and experiments in fluid mechanics research will be examined by reviewing several differ-

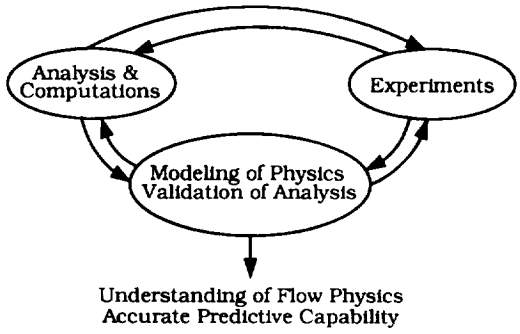

Figure 1 Schematic model of an integrated approach to fluid mechanics research.

ent investigations in which each approach has been used in varying degrees. This topic has been discussed by several previous authors. Dunham [1] and Lakshminarayana [2] have recently examined the role of computations in fluid mechanics research directed at turbomachinery. At the 2nd World Conference on Experimental Heat Transfer, Fluid Mechanics and Thermodynamics, Bergles [3] discussed the role of experiments in fluid mechanics research. In a review which addressed both analysis and experiments, Horlock [4] has pointed out that there are really six possible interactions between theoretical (T), computational (C) and experimental (E) research, which he labelled as the T/C, C/T, T/E, E/T, C/E, and E/C interactions.

In place of Horlock's "theoretical" category, I would like to introduce the concept of flow physics modelling. Flow physics models are simplified mathematical representations of real flow physics. These models are tightly coupled to both experimental and computational research. The formulation of such models is often based upon observations drawn from experimental measurements. The models serve to simplify the computational approach to a particular problem because the flow physics which they account for does not have to be solved computationally. A classic example of flow physics modelling is the turbulence modelling approach used in the solution of the Reynolds-averaged Navier-Stokes equations, wherein turbulent mixing is modelled as a simple diffusion process.

I believe that a modern approach to research in the fluid and thermal sciences should be structured as shown in Figure 1. The key feature of such an approach is the close interaction between experimental, analytic, and modelling disciplines. The benefits which can be realized from such an approach will be demonstrated by reviewing several research efforts in which the degree of coupling between the three disciplines varied. In reviewing these examples, a case will be made for the fact that modern fluid mechanics research can reap substantial benefits from a strong interaction between analysis, computations, and experiments. The design of two prototype computer systems which foster a close interaction between the three disciplines will also be described.

BOUNDARY LAYER STABILITY — A STUDY OF INDEPENDENT INVESTIGATIONS

The first example which I would like to examine consists of several investigations dealing with the stability of laminar boundary layers to small disturbances. These investigations were carried out over a period of 40 years by different research groups. Taken as a whole, they represent what I call an "open loop" type of interaction between computations, modelling, and experiments in that much of the work progressed in serial fashion rather than concurrently. Before describing the separate investigations, a little background information is in order.

It is generally accepted that transition from laminar to turbulent flow within a boundary layer occurs in several stages. If the free stream disturbance levels are sufficiently small, they will excite the normal modes of the laminar boundary layer, which are often referred to as Tollmien-Schlichting (TS) waves. These waves are small-amplitude, two-dimensional disturbances whose behavior is described by the Orr- Sommerfeld equations [5]. If the TS waves decay, then the boundary layer will remain laminar and the flow will be "stable". If the TS waves grow sufficiently strong (an "unstable" situation), they can trigger non-linear disturbances which in turn can lead to the formation of turbulent spots and eventually to a completely turbulent flow. Understanding the stability of the boundary layer as evidenced by the behavior of TS waves is therefore an important component of understanding the larger phenomena of boundary layer transition.

The Orr-Sommerfeld equations are derived from the full Navier-Stokes equations by making several simplifying assumptions (see Schlichting [5]). One of these assumptions is that a flat plate boundary layer can be modelled as a parallel flow, i.e. that the streamwise velocity, U, is only a function of the distance normal to the plate, y, and is independent of the streamwise distance, x. This is obviously a good model when the length Reynolds number is large and the boundary layer is relatively thin, which is often the case.

Analytic solutions of the Orr-Sommerfeld equations were first achieved by Tollmien [6] and Schlichting [7] in the early 1930's. In 1940, a key experiment was performed in a flat plate boundary layer in air by Schubauer and Skramstad [8]. This team had designed and built a wind tunnel with very low turbulence intensity (0.02%) in order to study boundary layer transition. The low free-stream disturbance environment in this tunnel enabled them to detect TS waves which were triggered by free-stream disturbances. This discovery was accomplished using hot wire anemometers to measure the unsteady velocity within the boundary layer. In order to more easily study the TS waves, Schubauer and Skramstad then added

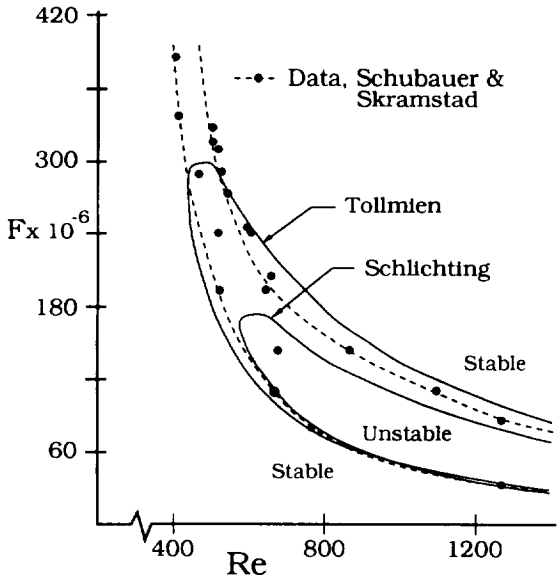

Figure 2 Comparison of analytically predicted boundary layer neutral stability characteristics [6,7] to measured neutral stability characteristics [8].

a thin vibrating ribbon placed near the plate surface to introduce small- amplitude two-dimensional harmonic disturbances into the boundary layer at known frequencies. They then mapped the growth and decay of these disturbances as they moved downstream and thus experimentally established the stability characteristics of the laminar boundary layer. Figure 2 is a comparison of their experimental results with the calculations of Schlichting and Tollmien. This figure is called a neutral stability diagram. The ordinate is the non-dimensional frequency of the disturbance and the abscissa is the displacement thickness Reynolds number. The solid lines in Figure 2 are the analytical solutions, while the broken lines are curves fared through the neutral points measured by Schubauer and Skramstad. The data points and analytical results define the neutral points of the boundary layer, which are the loci of disturbances that neither grow nor decay. The boundary layer is stable to disturbances which fall outside the neutral curve (in other words these disturbances will decay). The boundary layer is unstable to disturbances which fall inside the neutral curve - these disturbances will grow and are therefore potentially dangerous in that they can lead to transition.

The agreement between experiment and theory shown in Figure 2 was taken to be quite good by Schubauer and Skramstad. The agreement between theory and experiment at frequencies below 180 is clear. Although the analytic solutions do not agree with one another at low Reynolds numbers, they do bracket the experimental data. In addition, Schubauer and Skramstad noted that the unstable disturbances which they found at low Reynolds numbers and high frequencies were extremely weak and difficult to measure, which lead to larger experimental uncertainty in the (Re, F) coordinates of the neutral points in this region in Figure 2. Based on the agreement between measured and predicted results for several other characteristics of the disturbances, Schlichting himself declared in his textbook that "The experimental results show such complete agreement with the theory of stability of laminar flows that the latter may now be regarded as a verified component of fluid mechanics" [5].

During the 1950's and 1960's the solution of the Orr-Sommerfeld equations was further pursued using analytic approaches and, with the aid of computers, finite-difference techniques as well. These solutions were discussed by Jordinson [9], who also solved the equations numerically on a computer. The maximum unstable frequencies and the lowest Reynolds number for which the boundary layer is unstable, (termed the minimum critical Reynolds number, Re_{mc}) are summarized in Table 1 for a number of these investigations. Since the numerical solutions obtained by several additional investigators all gave exactly the same results, there was a general feeling that the numerical solutions were more accurate than the earlier analytic solutions of the Orr-Sommerfeld equation.

Table 1 Comparison of measured and predicted properties of the neutral stability curve at low Reynolds number.

Source	*Approach*	Re_{mc}	$F_{max} x10^{-6}$
Tollmein, 1931	Analytic	420	< 300
Schlichting 1933	Analytic	575	178
Lin, 1945	Analytic	425	345
Shen, 1954	Analytic	425	345
Wazzan, 1968	Numerical	520	245
Jordinson, 1970	Numerical	520	245
Schubauer 1940	Exp	400	400

Jordinson was one of a team of researchers at the University of Edinburgh who were performing an integrated experimental and computational investigation into why the computed and measured stability characteristics were different at low Reynolds numbers. In another phase of the computational effort, Barry and Ross [10] added terms to the Orr-Sommerfeld equation which accounted for the growth of boundary layer thickness with streamwise distance and used a modified version of Jordinson's program to numerically solve the equations. In so doing, they hoped to determine if the parallel flow assumption was invalid at low Reynolds numbers and thus the cause of the

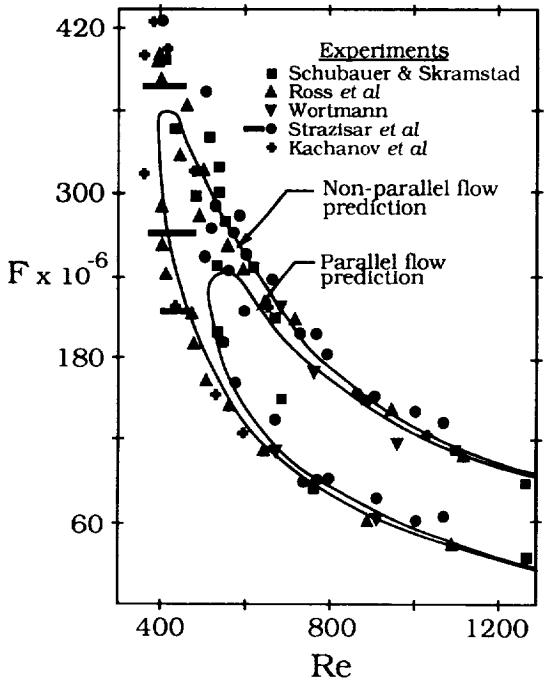

Figure 3 Comparison of measured boundary layer neutral stability points to the neutral stability curves determined using parallel and non-parallel flow calculations [13].

observed discrepancy. In the experimental effort, Ross et al. [11] repeated Schubauer and Skramstad's experiment. The numerical results displayed only a slight difference when the non-parallel effects were included — Re_{mc} was reduced from 520 to 500 and F_{max} increased from 245 to $260x10^{-6}$. On the other hand, the experimental results were in complete agreement with those of Schubauer and Skramstad. At this point, the cause of the experimental and numerical discrepancies was still unresolved.

In the early 1970's, several additional, independent experimental and numerical efforts followed. Each new experimental investigation verified the fact that the minimum critical Reynolds number for a flat plate laminar boundary layer is $Re_{mc=}$ 400. This body of evidence spurred continuing efforts to understand this phenomena from a theoretical point of view. Significant progress was finally achieved by Saric and Nayfeh [12,13] who included *all* of the non-parallel flow terms in the governing equations and then solved the equations using the method of multiple scales. Their analytic results with the non-parallel terms included and neglected are compared to the experimental results from five independent investigations in Figure 3. When all non-parallel effects are included, the calculated minimum critical Reynolds number is 400. From this comparison it is evident that the parallel-flow model, adopted almost forty years earlier in order to make the analytic solution of the governing equations tractable, was too restrictive at low Reynolds numbers. In retrospect, the earlier attempt to include non-parallel effects made by Barry and Ross had failed because they had included only *some* of the non-parallel effects.

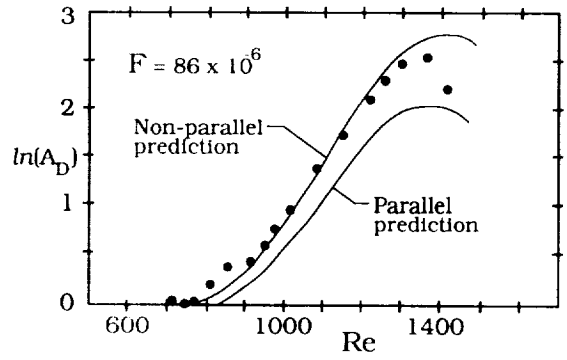

Figure 4 Comparison of measured and calculated growth of a disturbance of frequency $F=86x10^{-6}$ as a function of streamwise distance [13].

The results shown in Figure 3 might lead one to conclude that non-parallel effects are only significant at low Reynolds number and high frequency, since the parallel and non-parallel neutral curves are quite similar for disturbance frequencies less than $F=120x10^{-6}$. Further evidence that the non-parallel effects are important even at higher Reynolds numbers can be seen in Figure 4, which compares the predicted and measured log of the disturbance amplitude for a frequency of $F=86\ x10^{-6}$ as a function of streamwise distance (expressed as the displacement thickness Reynolds number). Note that the results in Figure 4 represent a cross-sectional cut through Figure 3 along a horizontal line at $F=86\ x10^{-6}$.

This example is representative of the way in which much or our fluid mechanics research is conducted. It represents a sound investigative approach in which analytic and experimental investigations were conducted by independent groups. Researchers learned from one another over time and achieved progress toward the ultimate goal of gaining insight into a particular aspect of fluid physics.

The experimental measurements, which were conducted in the actual non-parallel flow, ultimately showed that the attempt to "model" the boundary layer as a parallel flow was too restrictive. This fact was not immediately obvious for two reasons. First, the measurements departed from parallel-flow predictions in a region in which the measurements were difficult to acquire. There was therefore a lack of confidence in the early measurements which only disappeared when the measurements were verified during follow-on independent investigations. Second, the early parallel-flow computational results were misleading because they agreed closely with one another, which was taken as a confirmation of the parallel-flow theory, when

in reality these results were the *correct* solution to the *wrong* problem (the parallel flow problem). There are two lessons to be learned here: experimentalists must establish confidence in their measurements and numerical analysts must assess the validity of their assumptions and flow physics models.

A final point to be made before moving on is that the integrated experimental/numerical research effort of the Edinburgh team did not lead to an explanation of the disagreement between the numerical and experimental results. Therefore, although a tightly integrated attack on a problem can speed the transfer of information between experimenters, modelers, and numerical analysts, an integrated approach will not in itself guarantee success.

TRANSONIC COMPRESSOR BLADE WAKES — A STUDY OF CLOSELY-KNIT INVESTIGATIONS

The next case to be studied also consists of several separate investigations. In contrast to the previous case, these investigations were carried out over a brief span of time by only two research groups which were in fairly close contact with one another. One of the main features of this case study is the balanced role played by experiments, modeling, and computations - the effort taken as a whole will be shown to be a strong example of the principle embodied in Figure 1. In this example, experimental measurements uncovered flow physics which were not expected to be present. A simple flow physics model was then developed to explain the observed results. Computational analysis, which was not performed until the end of the effort, further verified both the experimental and modelling results.

The two research groups involved in this effort were the MIT Gas Turbine Laboratory and the NASA Lewis Research Center. During the early 1980's these two groups were involved in applying advanced measurement techniques to transonic axial-flow compressor rotors. MIT was using high-frequency-response pressure probes and a dual hot-wire aspirating probe to measure time-resolved pressure and temperature distributions downstream of a number of different transonic rotors. NASA-Lewis was using laser anemometry to study flow phenomena within and downstream of a NASA-designed transonic fan rotor. MIT had previously investigated the NASA fan in a blowdown compressor facility at MIT and later made additional time-resolved pressure and temperature measurements downstream of the fan in the steady-flow compressor facility at NASA-Lewis while the laser anemometer measurements were being acquired.

In a fixed frame of reference, the flow in a rotating blade row is always unsteady, with a periodicity set by the rotor rotational speed and the number of blades on the rotor wheel. In an isolated rotor case, in which there are no stationary blade rows located upstream or downstream

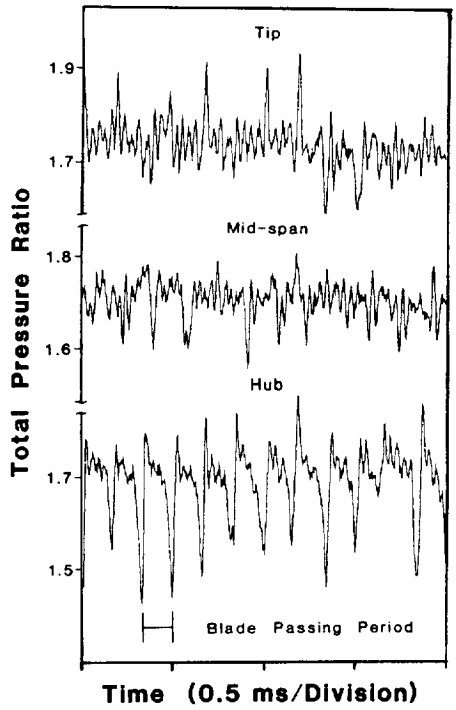

Figure 5 Instantaneous total pressure ratio measured at three spanwise locations downstream of a transonic axial-flow fan rotor [14].

of the rotor, the flow field within and around the rotor is expected to be steady in the rotor-relative reference frame (the frame of reference seen by an observer moving with the rotor). However, both MIT and NASA-Lewis discovered several unsteady flow phenomena in the NASA fan rotor when it was operated in an isolated-rotor configuration. The ensuing investigation into the cause of these unsteady flows forms our second case study.

Ng and Epstein [14] pursued the analysis of the instantaneous pressure and temperature measurements acquired with the MIT high-response probes downstream of the fan in the NASA facility. The total pressure ratio measured at three spanwise locations is shown in Figure 5. The rotor had 22 blades, and Figure 5 therefore shows about one-half of a rotor revolution. There are several features of the unsteady pressure measurements which are noteworthy. We see that the rotor blade wakes are not always evident, especially near the tip and at mid-span. Near the tip the wakes sometimes appear as an excess in pressure rather than as a pressure deficit. Finally, there are fluctuations in the total pressure ratio in the "core" flow between the blade wakes, a region in which the flow should be rather uniform. When such time traces were averaged over many rotor revolutions, the rotor wakes became regular in shape and the core flow region displayed a relatively smooth pressure profile. This result indica

that the features seen in the instantaneous time traces were not steady in the rotor relative frame of reference and also that they were not due to geometric variations in the rotor blades. In addition, MIT found a lower-frequency modulation of the wake depth, with a period on the order of one rotor revolution. This modulation is most evident in Figure 5 in the measurements acquired near the rotor hub.

The unsteady core-flow pressure fluctuations occupied a fairly narrow frequency range of 15-20 Khz. Ng and Epstein reasoned that these pressure fluctuations might be caused by shock unsteadiness. They showed that a shock motion of only 0.3 mm would be required in order to generate the observed pressure fluctuations. In addition, the 15-20 Khz frequency range was close to the frequency at which vortices would be shed from the blade trailing edge if the wake momentum thickness was taken as the characteristic length in the Strouhal correlation for vortex shedding from bluff bodies. Ng and Epstein therefore further proposed that vortex shedding from the blade trailing edge might be the driver for the shock unsteadiness. Although these proposals addressed the behavior of the core flow fluctuations, there was still no explanation for the large variation in the blade wake signatures shown in Figure 5.

In a concurrent investigation, my colleagues and I were acquiring laser anemometer measurements within and downstream of the fan rotor. By analyzing the distribution of velocities measured in the vicinity of the rotor shock, we were able to prove that the rotor shock was indeed unsteady, and that the shock moved over a distance of about 3 mm [15], thus verifying the unsteady shock

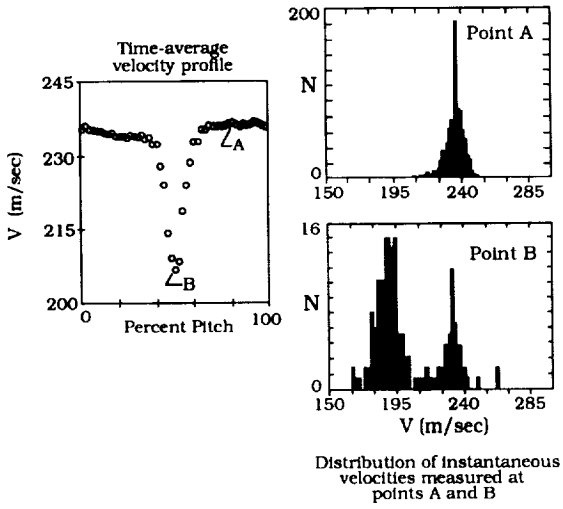

Figure 6 Time-averaged and instantaneous velocities measured with laser anemometry downstream of a transonic axial-flow fan rotor [16].

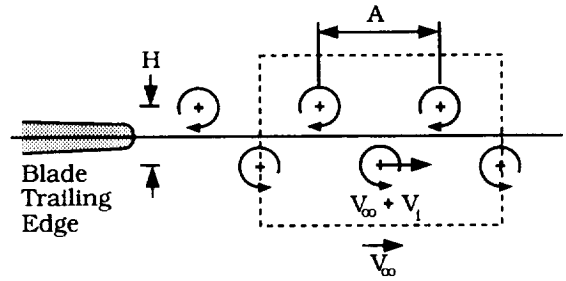

Figure 7 Schematic representation of the vortex street geometry used to model an axial-flow fan rotor wake [17,18].

behavior proposed by Ng and Epstein. A similar analysis of velocity measurements acquired in the wake [16] is shown in Figure 6.

The time-average wake velocity profile is shown in the left half of Figure 6. Each point in this profile represents the average of several hundred instantaneous velocity measurements acquired over many rotor revolutions. The probability density distributions (p.d.d.'s) of the instantaneous velocities measured at two different points, labelled A and B in the time-average velocity profile, are shown in the right half of the figure. The ordinate of each p.d.d. is the number of measurements which occurred in a velocity range which is 3 m/sec wide. The abscissa of each p.d.d. is the velocity in m/sec. The time-average velocity at points A and B is simply the arithmetic mean of all of the instantaneous velocity measurements acquired at each point.

At point A, which is in the core flow region between wakes, the instantaneous velocities display a single-moded, Gaussian-like distribution about the mean velocity value of about 240 m/sec. This behavior is characteristic of a steady, turbulent flow. However at point B, which is near the center of the wake, the instantaneous velocity measurements indicate the presence of two distinctly different velocity states. One of these states is centered at the core flow velocity of about 240 m/sec, while the other state is centered at a velocity near 190 m/sec. Looking at the time-average velocity profile, we see that the instantaneous velocities which fall in this lower-velocity state are well below the lowest time-average velocity in the center of the wake. These striking results indicated that the wake was not formed by the confluence of the boundary layers from the two rotor blade surfaces, but rather was the time average of two very different velocity states, one of which was the free- stream velocity and the other of which was a velocity well below the lowest time-average velocity. This behavior qualitatively matches that of a mean flow which is convecting vortices past the laser anemometer measurement point.

Based on this result, Jeff Gertz, a graduate student at MIT, formulated a wake model consisting of two staggered rows of Rankine vortices of opposite sign [17,18]. This model is shown schematically in Figure 7. The vortices consisted of an inner region of forced-vortex flow and an outer region which modeled the irrotational flow field of a classical Karman vortex street. Various model parameters were adjusted to yield a best-fit to the wake mean velocity profile measured by the laser anemometer. The shedding frequency value which produced the best fit was 16 Khz. This value corresponded closely to the shock oscillation frequency inferred by Ng and Epstein from the core-flow pressure fluctuation frequency, thus lending credence to their proposal that vortex shedding was driving the shock oscillation.

Gertz also modelled the high-response pressure probe measurement process by randomly sampling the model flow field while taking into account the rotor rotational speed and the convection of the vortices at the average rotor exit flow angle. A comparison between the measured instantaneous total pressure ratio and one predicted by sampling the vortex street model is shown in Figure 8. The model clearly predicts the pressure deficits and excesses which occur when vortices in the blade wake randomly impact on the high-response pressure probe as the blade wake rotates past the probe location.

At this point the two research groups had explained or measured unsteady core-flow pressure fluctuations, unsteady rotor shock motion, the presence of a vortex street in the blade wake, and an apparent coupling between the vortex shedding and the shock motion. All of this work had been accomplished through analysis of measurements

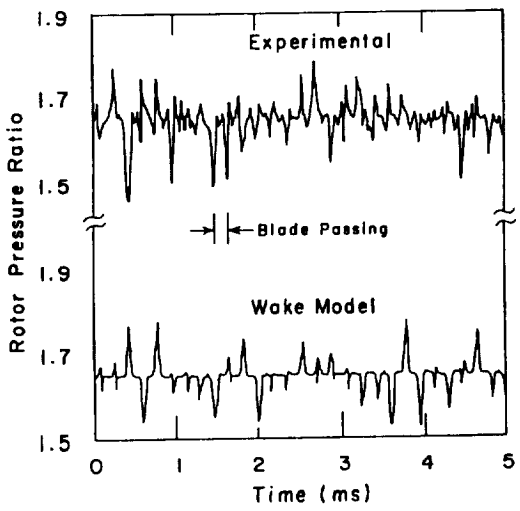

Figure 8 Comparison of measured instantaneous total pressure ratio in the fan rotor wake to that predicted from the vortex street model [16].

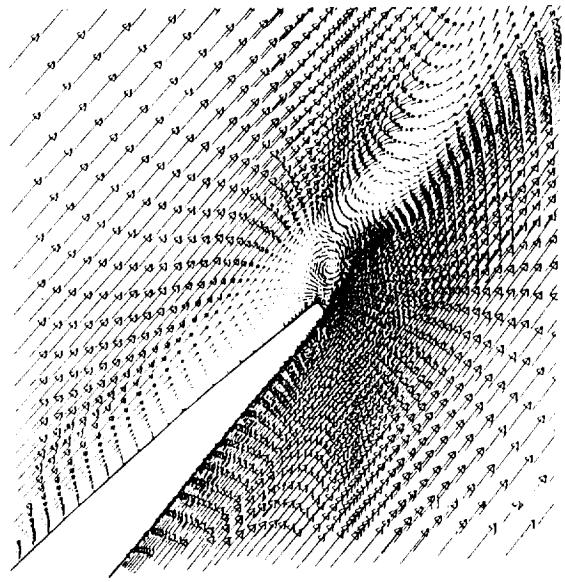

Figure 9 Instantaneous velocity field calculated near the trailing edge of a transonic axial-flow fan rotor showing separated flow near the blade suction surface and the presence of vortices downstream of the blade [18].

and the formulation of the relatively simple vortex street flow physics model. In a final effort, MIT conducted a two-dimensional, time-accurate Navier-Stokes calculation on the mid-span section of the fan rotor airfoil and found that vortex shedding could be predicted numerically [18,19]. However, the numerical results indicated that the mechanism of vortex shedding was not that of the classical Karman vortex street which results from the instability of two initially parallel free shear layers (which in this case would be formed by the separation of the blade surface boundary layers from the blade trailing edge). Instead, the results indicated that the suction surface boundary layer separated far from the blade trailing edge while the pressure surface boundary layer remained attached. The vorticity in the separated region on the suction surface rolled up into discrete vortices which were then shed from the blade suction surface into the blade wake. A velocity vector plot showing the separated region near the trailing edge as well as two vortices in the wake is shown in Figure 9. The calculated results further showed that the separation point moves along the suction surface at a frequency which is about one-half of the rotor rotational frequency. There was also some evidence that the rotor shock was moving, although this was hard to accurately discern due to the coarseness of the computational grid in the vicinity of the shock. The numerical results further showed that movement of the separation point causes a modulation in the strength of the shed vortices which in

turn causes the modulation in rotor wake depth which was noted in the near-hub measurements shown in Figure 5.

In summarizing this case, we see that experiment, modelling, and computation each played a major role in the final results. The string of investigations started with the observation of unexpected flow physical behavior in the high-response pressure and temperature measurements, in the laser anemometer measurements near the rotor shock, and in the laser anemometer measurements in the rotor wake. The laser anemometer measurements in the wake were used as a basis for formulating a physical model of the wake as the time-mean signature of a vortex street. The validity of this model was established by its ability to predict the salient features of the high-response probe measurements in the blade wake. Finally, a computational investigation was undertaken to further establish the validity of the vortex street model. The computational results showed that the shedding mechanism was not that of a classical shear layer instability and further explained the low-frequency oscillations observed in the experimental pressure measurements.

Although the MIT and NASA-Lewis research teams worked independently during the course of these efforts, there was a high degree of communication between the two groups. As in the first case studied, this effort also represents an "open loop" type of interaction between computations, modelling, and experiments in that much of the work progressed in serial fashion rather than concurrently.

CENTRIFUGAL COMPRESSOR FLOW PHYSICS — AN INTEGRATED INVESTIGATION

The last case to be studied utilized the integrated research approach embodied in Figure 1. Several aspects of this effort set it apart from the first two cases studied. First, computational investigations were performed *before* any experimental measurements were made in order to help plan the experiment. Second, the experimental results were used to refine numerical predictions while the experiment was in progress. This represents a "real-time feedback " type of interaction between experiments and computations. Finally, the experimental and numerical results were used in a complementary manner to develop an understanding of the flow physics.

The pre-test computational results were used to guide the design of experimental hardware to ensure that certain undesired flow features would not occur. Existing research hardware was actually modified during this part of the investigation. These computational results also helped the experimental researchers to develop an understanding of the flow field, which in turn helped them to plan the locations in which to concentrate their measurement effort. While the experiment was in progress, the computational grid was refined based on differences which were observed between the pre-test computations and early experimental results. These differences also guided changes to the parameters in a flow physics model which was part of the computation. This "real-time" interaction between the experiment and the computations significantly improved the accuracy of the computational results. During post-test analysis, the experimental results were used to further verify the accuracy of the computational results. Having established confidence in the numerical results, they were used to "fill in" flow field features in areas where experimental measurements were difficult to acquire.

The research effort described below was conducted by a single group at NASA-Lewis and involved the investigation of the viscous flow field within a large size, low-speed centrifugal compressor. Centrifugal compressors employ long, highly-curved blade channels. The blade channel curvature and high rotational speed of these compressors result in the generation of strong secondary flows within the blade channels. These secondary flows transport fluid which has low momentum and high total-pressure loss away from the channel walls and into the main-stream, which in turn impacts the compressor aerodynamic efficiency. A more detailed understanding of the generation and transport of secondary flows has therefore been the focus of many experimental and computational investigations of centrifugal compressor flow fields. Many of the earlier experimental investigations were unable to provide details of the viscous flow regions near the channel walls due to the small size of these regions in full-scale, high-speed centrifugal compressors. A unique large-scale, low-speed centrifugal compressor (LSCC) facility was therefore designed and built at NASA-Lewis for use in obtaining detailed laser anemometer flow field measurements within centrifugal impeller blade channels. The LSCC impeller was designed to be aerodynamically similar to full-scale impellers to insure that its secondary flow field would be an accurate representation of those found in full-scale impellers [20].

Three different three-dimensional viscous computational analyses were applied to the LSCC before starting to acquire laser anemometer measurements in order to develop an understanding of the LSCC flow field. All three of these analyses indicated the presence of a large separation in the diffuser located downstream of the impeller. A meridional (side) view of the velocity vector field calculated by one of these analyses [20] is shown in Figure 10 on a plane located mid-way between two impeller blades. The broken line marks a region of backflow which originates within the impeller, grows along the front wall of the diffuser, and extends all the way to the exit of the computational domain. The presence of backflow at the exit of the diffuser represents an undesirable boundary condition for most numerical schemes because the backflow cannot be specified *a priori*, but rather evolves during the computation. In fact, this computational solution did not

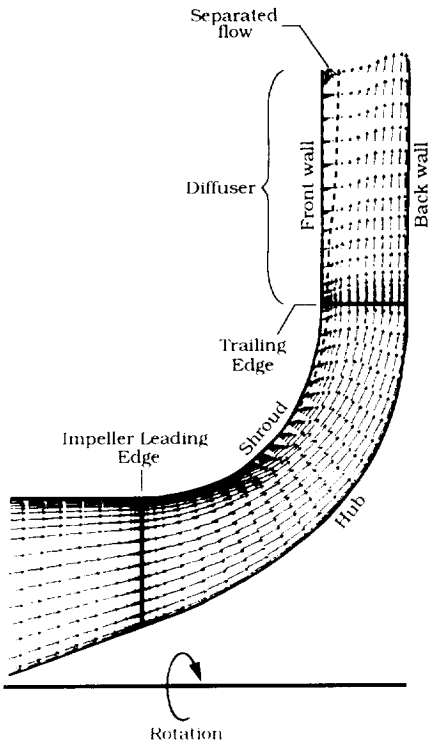

Figure 10 Meridional view of the predicted velocity field in the NASA low speed centrifugal compressor with a large impeller tip clearance gap showing front-wall separation in the diffuser [20].

converge until the diffuser was artificially contracted by altering the computational grid in order to reduce the flow area and thus eliminate the backflow. Preliminary total pressure measurements acquired near the impeller exit did not detect separated flow but did indicate a region of very low streamwise momentum near the front shroud wall. Since the LSCC was designed to provide detailed flow field measurements of high quality for use in assessing 3D Navier-Stokes analyses, it was considered undesirable to have a separation in the diffuser which might alter the impeller flow field and also produce an undesirable downstream boundary condition for numerical analyses.

The computational results indicated that the separation shown in Figure 10 was due to a large region of low-momentum fluid near the impeller shroud. This region was fed by fluid which leaked through the tip clearance gap between the moving impeller blades and the stationary shroud. The tip clearance gap was therefore reduced by a factor of two by adding balsa wood to the tip of each impeller blade. Computational analysis of the modified impeller was initiated as the impeller was re-installed in the test facility. Details of the predicted flow field near the inlet of the diffuser for the modified impeller are shown in Figure 11. A small separated flow region is still predicted

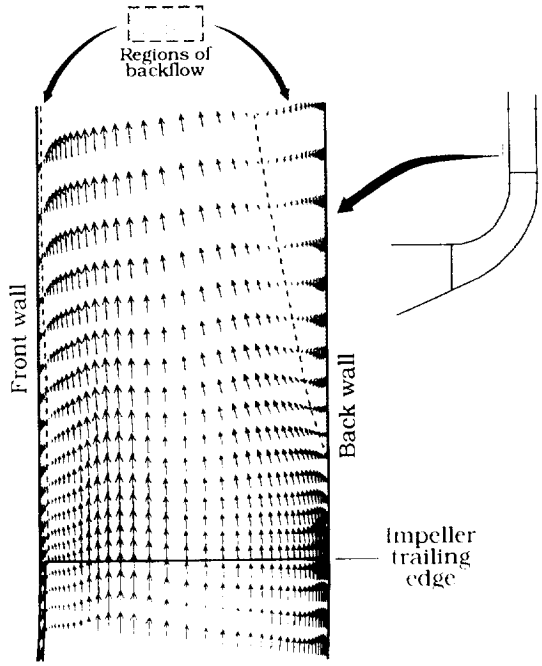

Figure 11 Meridional view of the predicted velocity field in the low speed centrifugal compressor with a reduced impeller tip clearance gap showing back-wall separation in the diffuser [20].

near the front wall of the diffuser. However, the most striking feature shown in Figure 11 is the presence of a large separation near the back wall of the diffuser. The predicted back-wall separation was verified by tufts and oil-flow visualization in the test facility. This new back-wall separation had apparently been suppressed in the earlier case due to the large front-wall blockage, which forced high-momentum main-stream flow toward the back wall.

The large back-wall separation was eliminated by modifying the back wall of the diffuser. One of the three-dimensional Navier-Stokes solvers used to generate the results shown in Figures 10 and 11 was used to guide the design of the new back-wall shape. The predicted velocity vector field for the final design is shown in Figure 12. The predicted results indicated that there would be no separation on the back-wall of the diffuser and that there would still be a slight separation very close to the front wall of the diffuser. A new diffuser back wall having the shape shown in Figure 12 was therefore fabricated and installed in the facility. Tuft and oil flow visualization once again confirmed the accuracy of the numerical predictions and the acquisition of detailed laser anemometer measurements within the impeller was therefore initiated. It is important to note that at this point in the investigation the viscous flow computations had been successfully used

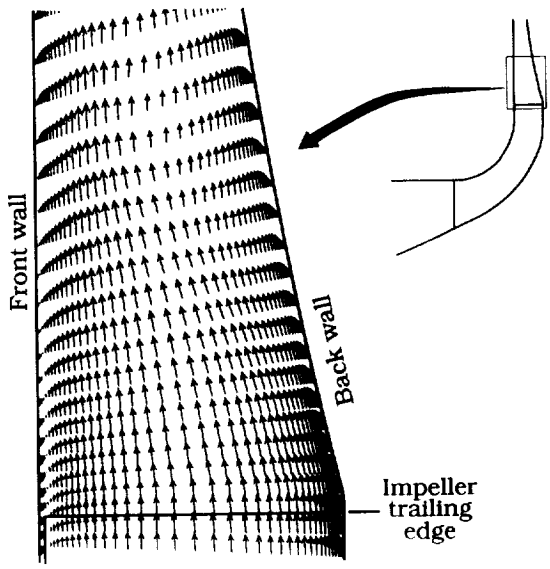

Figure 12 Meridional view of the predicted velocity field in the low speed centrifugal compressor with a modified diffuser back-wall showing separation—free flow in the diffuser [20].

to guide *two major modifications* to the test hardware *before a single detailed velocity measurement was acquired.*

Two of the major accomplishments which distinguished the detailed measurement phase of this investigation from previous experiments were the ability to measure all three velocity components within the impeller blade channels and the ability to make measurements very close to the blade channel side-walls (i.e. the impeller blade surfaces). These accomplishments made it possible for us to study the secondary flow within the blade channels and to also study the transport into the main-stream flow of low-momentum fluid which originated near the blade surfaces.

Although the specific definition of secondary flow is somewhat arbitrary, we conceptually think of it as that portion of the total velocity vector which does not contribute to the throughflow velocity. In this investigation the secondary flow was defined as that component of the total velocity vector in the reference frame of the rotating impeller which was not aligned with the streamwise grid lines used in the computational analysis [21]. Since the computational grid was body-fitted to the impeller channel, this definition of secondary flow provides a close fit to the conceptual definition. It also insures that secondary velocities are identically zero along the hub, the shroud, and on the blade surfaces, since all of these surfaces are computational grid lines.

In order to obtain the clearest comparison between numerical and experimental results, the measured and predicted secondary flow fields were obtained by applying the same processing techniques to both the measured and predicted total velocity vectors. The computational results were interpolated to the same locations at which measurements were taken before being displayed to further enhance the direct comparison between measured and predicted results. Appropriate checks were applied to this process to insure that the character of the predicted flow field was not altered by the interpolation process. In a similar manner, the computational grid directions were interpolated to the measurement locations for use in determining the measured secondary flow from the measured total velocity vector. Although these steps were not required in order to analyze the results, they greatly enhanced the ability to transfer information between the computational and experimental disciplines. The same conclusion has been drawn by other investigators who have performed similar research [22].

An example of the benefits which can be derived from such a process is shown in Figure 13. This figure is a direct comparison of the calculated and measured secondary flow on a cross-channel plane (plane J=135) which is located at 65% of the streamwise distance between the impeller inlet and exit. The computed secondary velocity vectors are shown in the left blade passage while the measured velocity vectors are shown in the right blade passage. Measurements were difficult to obtain in the lower portions of the blade channel and also near the tip of the impeller blade. The measured results are therefore only available at spanwise locations which range from 35 to 95% of the blade height. The computed results are displayed at 5% span increments across the full channel height, with additional computed results displayed at 98% and 101% of blade height. The location at 101% blade height actually lies in the clearance gap between the impeller blade tip and the impeller shroud.

One of the first features to be noted in Figure 13 is the fact that the computed results can be used to extend the measured results into spanwise locations at which measurements could not be acquired. This "extrapolation" is only valid if the computed and experimental results display good agreement in those regions of the flow field in which they can be directly compared to one another. In the present case there is good agreement between measurements and calculations below mid-span. Based on the calculated results in the lower half of the blade channel, we can therefore assume with some confidence that there are no strong secondary flow effects near the hub at this streamwise location, even though measurements could not be acquired in this region.

The computed results were also used to enhance the experimental results near the tip of the blade. Both computed and measured results in Figure 13 indicate that the flow near the blade suction and pressure surfaces (denoted as SS and PS respectively) migrates outward toward the

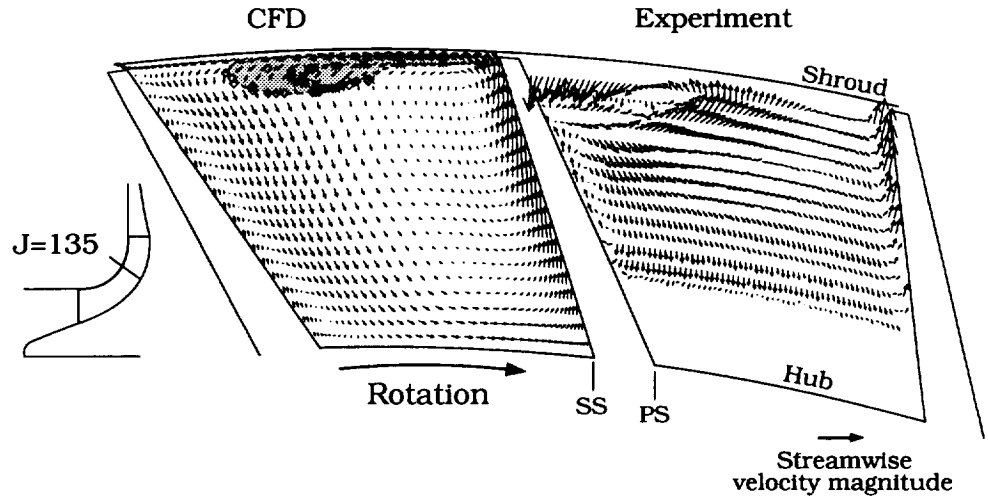

Figure 13 Cross-channel view of the secondary flow field in the low speed centrifugal compressor at station J=135. Numerical predictions in the left passage, laser anemometer measurements in the right passage [21].

blade tip. Since the experimental measurements do not extend beyond 95% span we cannot say with certainty, based only on the experimental results, what happens to this flow near the tip of the blade. However, one would expect that the flow continues to move toward the tip and becomes entrained in the tip clearance jet which exists in the gap between the blade tip and the impeller shroud. That this is indeed the case was verified by performing streamline tracking of fluid near the blade surfaces in the computed flow field. The diamond and asterisk symbols shown near the shroud in the computed results mark the location of streamline tracer particles which were released in the computation along the entire blade span at the blade leading edge. The diamond-shaped particles were released on the pressure surface of the blade which is in the center of Figure 13, while the asterisk-shaped particles were released on the suction surface of this blade. All of the fluid in the shaded region bounded by these particles originated near the blade surfaces. The tracer results clearly indicate that fluid originally located near the blade surfaces is swept into the tip clearance flow, which then migrates toward the pressure side of the blade channel near the blade tip.

One flow feature which does not display good agreement between the measured and calculated results is the vortical flow near the pressure surface/shroud corner of the impeller blade passage. The measurements display a much stronger secondary flow field in this region than do the calculations. This observation triggered an investigation into the tip clearance model used in the computation. The numerical scheme did not include a detailed grid in the clearance gap, but rather modelled the flow in this region as a jet issuing through a sharp-edged orifice [23]. The amount of mass-flow through the clearance gap was controlled by a discharge coefficient which accounted for the vena-contracta formed as the clearance jet crossed the sharp edge formed by the blade pressure surface and blade tip. A discharge coefficient of 0.6 was used in the result shown in Figure 13. When the disagreement between the computed and measured strength of the tip clearance flow was observed, the discharge coefficient was varied between 0.6 and 1.0 in an attempt to improve the predicted strength of the tip clearance flow. The unpublished results of these computations indicated that the predicted results could indeed be improved by using larger discharge coefficients.

Observed differences between measured and predicted flow features were also used to make several adjustments to the computational grid in order to improve the accuracy of the numerical results. Grid density was increased near the blade surfaces in order to more accurately calculate the large migration of fluid toward the tip of the blade that was seen in the measured results. The streamwise grid density was also increased near mid-chord when the experimental measurements indicated that the clearance flow was rapidly crossing from the suction to the pressure side of the passage in this region.

In summary, this investigation exemplifies the changing roles of the experimental and computational disciplines in several ways. Computations were conducted prior to the start of the experiment to provide the experimentalists with an understanding of the complex flow field which they were about to investigate. These computations predicted undesirable features in the flow field generated by the re-

search hardware and played an important role in guiding design changes in the hardware. The detailed experimental investigation and a continuing computational investigation were conducted concurrently and information was transferred between the two efforts in "near real-time". Through this information exchange, differences between predicted and measured features of the tip clearance flow were used to guide the selection of parameters in the tip clearance model used in the computational scheme and to guide the selection of parameters which controlled the computational grid. Finally, experimental and computational results were used in a complementary fashion to provide insight into the flow physics.

INTEGRATED COMPUTATIONS AND EXPERIMENTS (ICE) — A LOOK TOWARD THE FUTURE

The time scale over which experimental, modelling, and numerical analysis disciplines interact is constantly shrinking. In the boundary layer stability example, the interaction time scale was measured in decades. The fan rotor wake investigations spanned a total time period of just a few years. During the centrifugal compressor research effort, the interaction time shrank even further. In the facility modification phase of the effort, hardware changes were made within a few months after the computational results were completed. During the detailed measurement phase of the effort, laser anemometer measurements were often plotted within a day or two after they were acquired, and parameters in the computational analysis were changed almost weekly in response to differences observed between the measurements and the numerical predictions. Several highly-qualified researchers must work full-time in order to maintain such a pace. Although computers certainly aid both the experimentalist and the numerical analyst, the researchers must still assimilate a vast amount of information and then rapidly make decisions in order to keep the investigation moving forward. Research engineers can be freed from this time—consuming process by using computers to speed the comparison of experimental and numerical results and to make some decisions for us. In this section of the paper we will look at two recent efforts aimed at meeting this goal. Before we proceed I would like to discuss two practical problems which can be alleviated by using computers to enhance the acquisition and analysis of data.

Simply stated, the first problem is "Where should I concentrate my measurements in order to capture the relevant physical features which exist in this flow field?" While a coarse measurement grid will certainly provide a global view of the flow field features, many important flow phenomena may not be captured. A classic example of this dilemma is the flow in a channel which has thin boundary layers. If the boundary layer thickness is 5% of the channel width, then measurements made every 10% of channel width would completely miss the boundary layer. The question of "Where do I measure?" is currently addressed by performing a pre-test analysis of the flow field, and then having a research engineer manually create a measurement plan based on knowledge gained from the predictions. Through such a process we first learn how thick the boundary layer is, then create a measurement grid which will cluster measurements within the boundary layer if that is the main feature of interest to us.

The second practical problem faced by an experimentalist is the fact that the investigation of a particular flow field feature often cannot be completed during a single research run. This is due in part to not knowing where to measure and in part to the fact that detailed measurements require a significant amount of time. The researcher is therefore faced with having to acquire a consistent set of measurements across several research runs in the test facility. When this situation occurs one must make sure that the operating conditions are duplicated as closely as possible from run-to-run, which is not always easy to do. For example, in our transonic compressor research facility we often spend at least one hour of each research run insuring that we are at the same operating condition we had on the previous run. This problem could be alleviated if we could increase our measurement efficiency, thus acquiring more data during each research run.

The first effort I would like to discuss that attempts to use computers to help us make decisions was recently conducted at the NASA-Ames Research Center [24]. This effort addresses the issue of measurement efficiency and the question of "Where do I measure?" by using a rule-based computer program to control the acquisition of five-hole pressure probe measurements in a wind tunnel. When given a preliminary set of wind tunnel test data and a simple numerical model of the flow field being measured, the control program uses the data acquired so far to decide where to make the next measurement, then commands the tunnel data acquisition system to move the probe to that location and acquire a data point. Through this process the control program "homes-in" on flow features of interest.

The system has been demonstrated in an application in which vortex generators were used to create three streamwise vortices in a wind tunnel. An initial manually-controlled survey of the wind tunnel test section on a coarse (6x12 point) mesh was used to roughly identify the centers of the three vortices. A numerical model of the vortex flow field was then fit to the data and supplied to the control program. A set of "if-then" rules was also written for the control program to use while guiding a more detailed flow field survey. These rules enabled the control program to command large probe position changes between measurement points in areas of the flow field in which the velocity gradients were low, and finer position changes in areas where the velocity measurements indicated that a vortex was present. The measured secondary

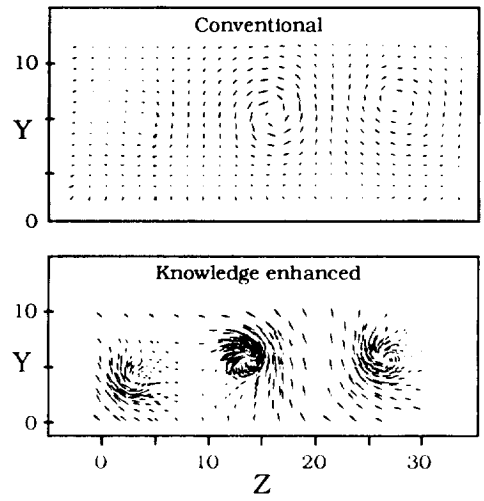

Figure 14 Comparison of flow field measurements acquired at uniformly-spaced locations to those acquired at locations chosen by a knowledge-based control program [24].

velocity vectors which resulted from this "knowledge enhanced" survey are compared to those measured during a uniformly spaced "conventional" survey in Figure 14. The "conventional" survey is typical of the approach one would use if prior knowledge of the flow field was not available. The number of measurement points in the "conventional" survey was 375 and the number in the "knowledge enhanced" survey was 440. The improvements which result from the "intelligent" placement of data acquisition points are obvious — many of the points in the conventional survey tell us very little about the vortices.

Such techniques hold great promise for maximizing the use of test facility time, which is an especially important consideration for facilities with large operating costs. The challenge in implementing this strategy on a wider basis lies in the ability to construct control software capable of handling more complex flow fields. In addition, it is not clear that such a system will ever be capable of "discovering" flow features which are not predicted by a pre-test computational model. For example, if we study Figure 13 we see that although the CFD results would guide us to make measurements near the blade surfaces where significant migration of fluid toward the tip of the blade is predicted, these same results would not lead us to expect the large streamwise vortex which appears in the measurements near the pressure surface/shroud corner of the passage.

Another effort aimed at using computers to help us make decisions is currently underway at the NASA-Lewis Research Center [25,26]. The project titled Integrated CFD and Experiments (ICE), utilizes parallel computing and advanced workstation technology to reduce the time

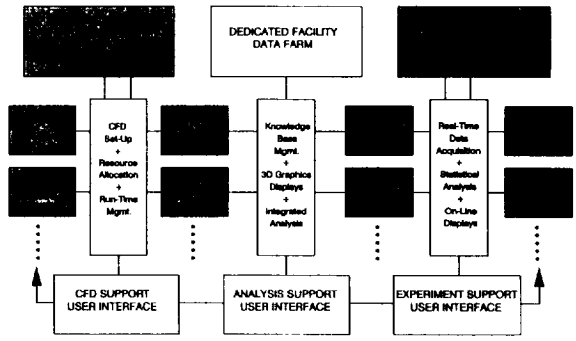

Figure 15 Schematic of the ICE computer system architecture [25].

and effort required to transfer information between experimental and computational disciplines. The prototype computing environment being developed by the ICE project team consists of three subsystems as shown schematically in Figure 15. One subsystem controls the acquisition, real-time analysis, and archiving of experimental data. This subsystem uses parallel computer architecture to speed data reduction, thus enabling us to display detailed measurements while a research run is in progress instead of waiting until the next day as is currently required. This capability will allow more detailed probing of flow features during a single research run, and will help alleviate the issues related to acquiring measurements across several separate research runs. A second ICE subsystem controls the execution of CFD codes across a distributed computing environment. This subsystem allows the researcher to monitor the progress of computational solutions on a variety of computing platforms which are networked to the ICE system. Through this subsystem the researcher can change parameters in a numerical solution, display results, and archive numerical results. The third ICE subsystem supports analysis of both numerical and experimental results. This subsystem uses knowledge-based management techniques to retrieve results which have been stored in a "data farm" by the other two subsystems. The analysis subsystem also utilizes standardized graphics visualization software which graphically displays experimental and computational results in identical formats such as that shown in Figure 13 in order to enhance knowledge transfer between experiments and computations. When fully operational, ICE will allow us conduct the type of research which was described in the Centrifugal Compressor example above in near real-time. In this scenario the researcher will be "in the loop" guiding the advance of both experiments and computations, but his workload will be significantly reduced through the application of standardized user interfaces, graphics visualization tools, and database management tools.

CONCLUDING REMARKS

One might ask "Can good research be conducted without having an interaction between experiments, flow physics modelling, and computations?" The answer of course is "Yes". Many investigations in fluid and thermal sciences have been and will continue to be conducted within a single discipline. However, there is much to be gained through the cross-fertilization which occurs within an interdisciplinary research team. Each member of the team has something which the others can use. The experimentalist has the data which the modeler needs to construct his models and the numerical analyst needs to assess the accuracy of his predictions. The numerical analyst can provide guidance to the experimentalist in designing his hardware and planning his measurements. The modeler constructs mathematical models for physical phenomena which are still too complex to compute, such as turbulence. But perhaps the most important item which each discipline brings into the team is its unique insight into fluid and thermal physics. The impact of insight cannot be understated. In the words of Wygnanski [27], "People used to have huge wind tunnels. What do you get out of them? Having a wind tunnel doesn't tell you what to do with it. Having a computer doesn't tell you what to do with it. The insight about what to do with a facility is the important thing. And it's still a human insight." I believe that the greatest possible insight is achieved when we use a multidisciplinary approach in our investigations.

NOMENCLATURE

A	Vortex spacing
A_D	Disturbance amplitude
F	Disturbance frequency
F_{max}	Maximum frequency for which a boundary layer is unstable
H	Vortex street width
J	Streamwise grid indice
N	Number of measurements
PS	Pressure surface
Re_{mc}	Minimum critical Reynolds number
SS	Suction surface
U	Streamwise velocity
V	Relative velocity
V_i	Vortex-induced velocity
V_∞	Free-stream relative velocity
x	Streamwise direction
y	Direction normal to a surface
z	Cross-channel direction

REFERENCES

1. Dunham, J., The Role of Flow Field Computation in Improving Turbomachinery in 15th ICAS Congress, London, pp. 967-980, September 1986.
2. Lakshminarayana, B., An Assessment of Computational Fluid Dynamics Techniques in the Analysis and Design of Turbomachinery - The 1990 Freeman Scholar Lecture, ASME J. Fluids Engr. 113, 315-352, 1991.
3. Bergles, A.E., The Role of Experimentation in Thermofluid Science, Exp. Thermal Fluid Sci. 3, 2–13, 1990.
4. Horlock, J.H., The Balance Between Theoretical, Computational, and Experimental Work in Turbomachines in Joint National Symposium on the Influence of Aviation on Engineering and the Future of Aeronautics in Australia, Melbourne, pp. 1-13, August 1985.
5. Schlichting, H., Boundary-Layer Theory, 6th Ed., McGraw-Hill, New York, 1968.
6. Tollmien, W., The Production of Turbulence, NACA TM 609, 1931.
7. Schlichting, H. Amplitudenverteilung und Energiebilanz der kleinen Storungen bei der Plattenstromung, Math. Phys. Klasse, Bd. I, 47–78, 1935.
8. Schubauer, G.B., and Skramstad, H.K., Laminar Boundary Layer Oscillations and Stability of Laminar Flow, NACA Report 909, 1948.
9. Jordinson, R., The Flat Plate Boundary Layer. Part I. Numerical Integration of the Orr-Sommerfeld Equation, J. Fluid Mech. 43, 801–811, 1970.
10. Barry, M.D.J., and Ross, M.A.S., The Flat Plate Boundary Layer. Part 2. The Effect of Increasing Thickness on Stability, J. Fluid Mech. 43, 813-818, 1970.
11. Ross, J.A., Barnes, F.H., Burns, J.G., and Ross, M.A.S., The Flat Plate Boundary Layer. Part 3. Comparison of Theory with Experiment, J. Fluid Mech. 43, 819–832, 1970.
12. Saric, W.S., and Nayfeh, A.H., Nonparallel Stability of Boundary-layer Flows, Phys. Fluids 18 945-950, 1975.
13. Saric, W.S., and Nayfeh, A.H., Nonparallel Stability of Boundary Layers with Pressure Gradient and Suction in Laminar-Turbulent Transition, AGARD CP-224, Copenhagen, pp. 6.1–6.21, May 1977.
14. Ng, W.F., and Epstein, A. H., Unsteady Losses in Transonic Compressors, ASME J. Engr. for Power 107, 345–353, 1985.
15. Strazisar, A.J., Investigation of Flow Phenomena in a Transonic Fan Rotor Using Laser Anemometry, ASME J. Engr. for Power 107, 427–435, 1985.

16. Hathaway, M.D., Gertz, J.B., Epstein, A.H., and Strazisar, A.J., Rotor Wake Characteristics of a Transonic Axial-Flow Fan, AIAA J. 24, 1802- 1810, 1986.
17. Gertz, J.B., Unsteady Design-Point Flow Phenomena in Transonic Compressors, Ph.D. Thesis, Dept. Aero. Astro., Mass. Inst. Tech., Cambridge, Ma., 1985.
18. Epstein, A.H., Gertz, J.B., Owen, P.R., and Giles, M.B., Vortex Shedding in High-Speed Compressor Blade Wakes, AIAA J. Prop. and Power 4, 236- 244, 1988.
19. Owen, P.R., Computational Simulation of Unsteady Flow in a Transonic Compressor Rotor, M.S. Thesis, Dept. Aero. Astro., Mass. Inst. Tech., Cambridge, Ma., 1986.
20. Hathaway, M.D., Wood, J.R., and Wasserbauer, C.W., NASA Low-Speed Centrifugal Compressor for Three-Dimensional Viscous Code Assessment and Fundamental Flow Physics Research, ASME J. Turbomachinery 114, 295- 303, 1992.
21. Hathaway, M.D., Chriss, R.M., Wood, J.R., and Strazisar, A.J., Experimental and Computational Investigation of the NASA Low-Speed Centrifugal Compressor Flow Field, ASME Paper No. 92–GT-213, 1992. To be published in ASME J. Turbomachinery.
22. Leylek, J.H., and Wisler, D.C., Mixing in Axial-Flow Compressors: Conclusions Drawn from Three-Dimensional Navier-Stokes Analyses and Experiments, ASME J. Turbomachinery 113, 139–160, 1991.
23. Dawes, W.N., Development of a 3–D Navier Stokes Solver for Application to all Types of Turbomachinery, ASME Paper No. 88–GT-70, 1988.
24. Cantwell, E.R., Zilliac, G., and Fukunishi, Y., An Intelligent Data Acquisition System for Fluid Mechanics Research, Exp Fluids 8, 233–236, 1989.
25. Szuch, J.R., Arpasi, D.J., and Strazisar, A.J., Enhancing Aeropropulsion Research with High-Speed Interactive Computing in 10th International Symposium on Air-Breathing Engines, Nottingham, pp. 286–298, September 1991.
26. Babrauckus, T.L., and Arpasi, D.J., Integrated CFD and Experiments Real-Time Data Acquisition Development, to be presented at the 38th ASME Gas Turbine & Aeroengine Congress and Exposition, Cincinnati, May 1993.
27. Wygnanski, I., The Future of Experimental Fluid Mechanics Research, Dantec Electronics Newsletter, 1988.